



## Research article

# *Ganoderma lucidum* polysaccharides reduce the severity of acute liver injury by improving the diversity and function of the gut microbiota

Xiao-tian Zhang<sup>a</sup>, Yue Yang<sup>b</sup>, Chunlei Ji<sup>b</sup>, Yujuan Fu<sup>b</sup>, Xinyi Pu<sup>b</sup>, Guangyu Xu<sup>b,\*</sup><sup>a</sup> Department of Clinical Laboratory, The Second Hospital of Jilin University, Changchun, Jilin, 130000, China<sup>b</sup> College of Pharmacy, Beihua University, 3999 Binjiang East Road, Jilin, Jilin, 132013, China

## ARTICLE INFO

## Keywords:

*Ganoderma lucidum* polysaccharides  
Intestinal flora  
Acute liver injury  
16S rRNA  
Inflammation  
Oxidative stress

## ABSTRACT

Acute liver injury (ALI) is an abnormal liver function caused by oxidative stress, inflammation and other mechanisms. The interaction between intestine and liver plays an important role in ALI, and natural polysaccharides can participate in the regulation of ALI by regulating the composition of intestinal flora. In this study, *Ganoderma lucidum* polysaccharide was used as the research object, and ICR mice were used to construct an acute liver injury model induced by carbon tetrachloride (CCl<sub>4</sub>). 16S rRNA sequencing technology was used to analyze the flora structure abundance and detect the changes of intestinal flora. The effective reading of 8 samples was obtained by 16S rRNA sequencing technology, and a total of 1233 samples were obtained. The results of alpha diversity analysis showed that the sequencing depth was sufficient, the abundance of species in the samples was high and the distribution was uniform, and the sequencing data of the samples was reasonable. Nine species with significant differences were screened out by abundance analysis of intestinal flora structure at genus level. Beta diversity analysis showed that species composition was different between the model group and the treatment group. *Ganoderma lucidum* polysaccharide can maintain the integrity of mucosal barrier by promoting the proliferation of intestinal epithelial cells and anti-oxidative stress injury, thereby improving the intestinal mucosal inflammation of mice, regulating intestinal flora, and effectively alleviating CCl<sub>4</sub>-induced acute liver injury.

## 1. Introduction

Acute liver injury (ALI) is a disorder of liver function caused by various mechanisms such as oxidative stress, inflammation, and hepatocyte apoptosis and necrosis [1,2]. It is a common pathological basis for various other liver diseases, and in severe cases, it can gradually progress to cirrhosis and liver cancer [3,4]. Studies have shown that intestinal flora has close connection with ALI [5,6]. When normal liver physiology is disrupted, certain bacterial components, such as lipopolysaccharide (LPS), enter the liver from the gut lumen through the portal vein, causing hyperinflammation that further damages tissue and exacerbates preexisting liver disease [7,8].

Natural product polysaccharides can participate in the regulation of ALI by regulating the composition of intestinal flora [9,10]. Many studies have reported that natural antioxidants, such as polysaccharides, ketones, glycosides, and alkaloids, are effective in

\* Corresponding author.

E-mail address: [xuguangyu2005@163.com](mailto:xuguangyu2005@163.com) (G. Xu).

inhibiting the liver disease caused by reactive oxygen species [11,12]. *Ganoderma lucidum* polysaccharides (GLP) is the main active ingredient of *Ganoderma lucidum* in the genus Porifera. Studies have shown that GLP possesses significant antioxidant, anti-inflammatory, immunomodulatory and hepatoprotective activities [13,14]. GLP can also modulate the function of gut microbiota and immune cells [15]. The combination of GLP and ciprofloxacin can treat salmonella infection, regulate the gut flora, protect the intestinal barrier, and increase the number of probiotics [16].

In this study, ICR mice were used to establish a model of carbon tetrachloride (CCl<sub>4</sub>)-induced acute liver injury. 16S rRNA sequencing technology was used to detect the changes of intestinal microbiota, and alpha diversity analysis and LEfSe analysis were used to screen the differential flora and related pathways of *Ganoderma lucidum* polysaccharide in mice with liver injury. Finally, the protective effect of *Ganoderma lucidum* polysaccharide on liver injury by improving the diversity of intestinal flora in mice was elucidated, which provided a theoretical basis for the further development and utilization of *Ganoderma lucidum* polysaccharide.

## 2. Materials and methods

### 2.1. Materials

The polysaccharide of *Ganoderma lucidum* used in the experiment was provided by the Laboratory of Drug Analysis, Beihua University (Jilin, China), *Ganoderma lucidum* polysaccharide was extracted by water extraction and alcohol precipitation. The yield of *Ganoderma lucidum* polysaccharide reached the maximum of 8.74 %, and the polysaccharide content was about 43.7 %. Anhydrous ethanol, and methanol (Liaoning Quanrui Reagent Co., Ltd., Jinzhou, China); CCl<sub>4</sub> (Shanghai Aladdin Biochemical Technology Co., Ltd., Shanghai, China); Paraformaldehyde (Changchun Huayi Biotechnology Co., Ltd., ChangChun, China).

### 2.2. Analysis of monosaccharide composition of GLP

Mixed standard solutions of mannose (Man), Gluconic acid (GlcA), rhamnose (Rha), galactose uronic acid (GalA), glucose (Glc), galactose (Gal), xylose (Xyl), arabinose (Ara) and fucose (FUC), and standard solutions of the above monosaccharides, respectively. The HPLC system was Shimadzu LC-20AT, SPD-20A UV-Vis Detector, and the chromatographic column was COSMOSIL 5C18-PAQ 4.6ID × 250 mm, the eluting agents of 80.8 % PBS (0.1M, pH7.0) and 19.2 % acetonitrile (v/v), the flow rate was 1.0 ml/min, the column temperature was 35 °C, and the injection volume was 10 µl.

### 2.3. Determination of molecular weight distribution of GLP

The molecular weight distribution of GLP was detected by HPSEC method. The chromatographic column was TSK-Gel G3000PWXL Column, with a column temperature of 40 °C, the eluent was 0.2 mol/L NaCl, and the flow rate was 0.6 ml/min, in which  $V_0 = 6.1632$  ml,  $V_t = 10.065$  ml,  $V_t - V_0 = 3.9018$  ml.

### 2.4. Animal experiments

Male, 18–22 g, ICR mice (Chang Chun Yisi Experimental Animal Technology Co., Ltd.), the mice were fed under conditions of 20–24 °C, 40–60 % humidity, free access to food and water, and the experiment began after the mice adapted to the laboratory feeding environment for 7 days. Mice were randomly divided into three groups: control group (CON), model group (MOD) and *Ganoderma lucidum* polysaccharide (GLP) treatment group. There were 8 mice in each group. The mice in GLP-treated group were gavaged with *Ganoderma lucidum* polysaccharide (300 mg\*kg<sup>-1</sup> BW day<sup>-1</sup>). The dose of the experimental drug is the common dose for adults, which is converted into the equivalent dose according to the human and mouse body surface area conversion formula, and prepared with distilled water to the required concentration before use [17]. The duration of administration follows the general duration of acute liver injury models [18,19].

GLP group was given 300 mg\*kg<sup>-1</sup> BW day<sup>-1</sup> ganoderma polysaccharides, CON and MOD groups were given an equal volume of distilled water for 7 consecutive days. Two hours after the last administration, mice in the MOD and GLP-treated groups were intraperitoneally injected with 1 % CCl<sub>4</sub> olive oil solution (10 ml/kg) [20]. After 24 h of fasting, the mice were put into an euthanasia box (connected to a carbon dioxide cylinder and flow controller), the concentration of input carbon dioxide was 100 %, and the flow rate of carbon dioxide was set at 20 % of the chamber volume/minute. After the respiratory arrest and eye color fading of the mice, the carbon dioxide was continuously input for 5 min, and then the mice were placed out the euthanasia box for 5 min to ensure the death of mice. we killed the mice under ether anesthesia. Blood samples were collected and serum was immediately separated. Liver tissue was isolated from each mouse and stored at –80C for further experiments.

### 2.5. Detection of biochemical indicators in the liver tissue and serum of mice

The eyeball blood and liver tissue homogenates were centrifuged at 3000 rpm for 15min at 4 °C, respectively, and the serum and liver tissue supernatant were separated. The activities of Alanine aminotransferase (ALT), aspartate aminotransferase (AST), glutathione (GSH), malondialdehyde (MDA), superoxide dismutase (SOD) and interleukin 17a (IL17A) Elisa kits (ABclonal, Wuhan, China) were detected according to the instructions of the kit. The OD value was measured by InfiteM200PRO multi-mode microplate reader (TecanCo, Ltd., Shanghai, China), and the biochemical indicators in serum and liver tissue were calculated.

## 2.6. Mouse feces collection

Defecation was promoted by massaging the abdomen of mice with finger pulp, and feces were collected with forceps after heat sterilization. The collected feces were placed in sterile EP tubes after autoclaving. Immediately collected samples stored in the refrigerator - 80 °C.

## 2.7. 16S rRNA sequencing

The total DNA of microorganisms in the stool samples was extracted using TopTaq DNA Polymerase kit according to the kit instructions. The integrity and quality were detected by agarose gel electrophoresis and Nanodrop 2000, respectively. The electrophoretic bands were clearly visible without obvious degradation. The concentration was  $\geq 20$  ng/ $\mu$ L, the total amount was  $\geq 500$  ng, and the OD<sub>260/280</sub> was 1.8–2.0. Amplification of the 16sRNA gene V3–V4 [21] was performed using the following primer pairs: 341F (5'-CCTACGGGNGCWGAG-3') and 785R (5'-GACTACHVGGGTATCTAATCC-3'). Specific tag sequences were introduced to the end of the library by high-fidelity PCR, and the library was precisely quantified by Qubit. The size of the sequencing library inserts was determined by an Agilent 2100 Bioanalyzer. Libraries were sequenced with a  $2 \times 250$ -bp double-end sequencing strategy using the Miseq platform [22].

## 2.8. Bioinformatics analysis

Sequences were clustered into operational taxonomic units (otus) based on 97 % sequence similarity. The representative sequences of OUT were analyzed by taxonomy and compared with the database for species annotation. And on the basis of Species classification at the level of Kingdom, Phylum, Class, Order, Family, Genus and species, Species composition, indicator species analysis, Alpha diversity analysis, Beta diversity analysis and community function prediction were performed.

## 2.9. Statistical analysis

Data were statistically analyzed using SPSS 17.0 software (SPSS, China). The data were expressed as mean  $\pm$  standard deviation (mean  $\pm$  SD) and tested by Analysis of Variance (ANOVA) Dunnett's multiple comparisons. A value of  $P < 0.05$  indicated a statistically significant difference.

## 3. Results

### 3.1. Monosaccharide composition of GLP

The monosaccharide composition of GLP was analyzed by HPLC (Fig. 1), and the results showed that GLP was mainly composed of

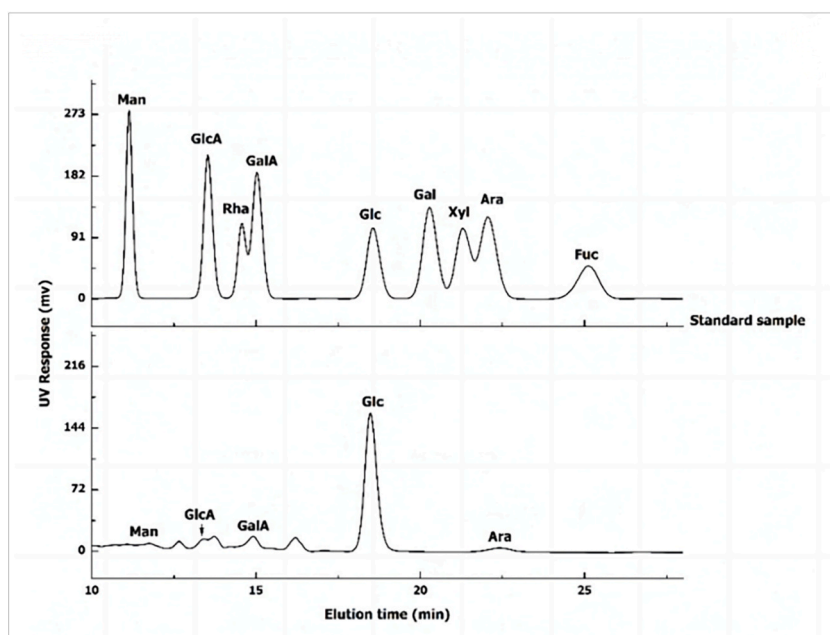


Fig. 1. Monosaccharide composition chromatography of GLP.

Man (2.9 %), GlcA (4.1 %), GalA (8.2 %), Glc (78.1 %), and Ara (6.7 %).

### 3.2. Molecular weight distribution of GLP

The results showed that 5 peaks of *Ganoderma lucidum* polysaccharide were eluted in HPSEC chromatography, and the average molecular weight was estimated to be 285, 13.6, 2, 0.2, 0.1 kDa, respectively (Fig. 2). The retention time and molecular weight of the various components are shown in Table 1.

### 3.3. Changes of biochemical indexes in mouse liver tissue

Biochemical index detection results showed (Fig. 3) that compared with CON group, AST, ALT, MDA and IL17A levels in MOD group were significantly increased ( $P < 0.01$ ), while GSH and SOD contents in liver tissue were significantly decreased in MOD group ( $P < 0.01$ ). Compared with MOD group, the levels of AST, ALT, MDA and IL17A in GL group were significantly decreased ( $P < 0.01$ ). The content of SOD in liver tissue of GL group was significantly increased ( $P < 0.01$ ).

### 3.4. OUT level analysis

We assessed the effect of drug administration on gut microbiota composition by high-throughput sequencing of the V3 + V4 region of bacterial 16S rRNA. OTUs classification was performed on the samples of the two groups of model group and *Ganoderma lucidum* polysaccharide treated group, and the unique OTU/ASVs in each group of samples and the common OTU/ASVs between groups were screened based on 97 % similarity for visual display, as shown in Fig. 8. Random sampling was performed, and a total of 1233 OUT of 8 valid readings were obtained. A total of 457 otus were obtained from 4 samples in the model group, and 325 otus were obtained from 4 samples in the *Ganoderma lucidum* polysaccharide administration group. A total of 451 otus were obtained from the two groups (Fig. 4).

### 3.5. Analysis of microbial $\alpha$ diversity

In order to reflect the microbial diversity of each sample at different sequencing quantities, we performed Shannon-Wiener diversity index curve analysis (Fig. 5A), and the curve tended to be flat. This result indicated that sequencing data amount could reflect the vast majority of microbial information in the sample. From the dilution curve, we can find that the curve flattens out with the increase of the number of extracted sequences, indicating that the amount of sequencing data of the sample is reasonable (Fig. 5B). Rank-abundance curve is a commonly used visual analysis method to evaluate species diversity, and the results show that the abundance of species in the sample is high and evenly distributed (Fig. 5C). Through the species accumulation box plot, we can find that with the increasing sample size, the curve tends to be flat, indicating that our sequencing depth is sufficient and the analysis is meaningful (Fig. 5D).

### 3.6. LEfSe analysis

In order to find the biomarker bacteria with statistical abundance differences between different groups, LEfSe analysis and LDA analysis were performed on the samples between groups. Fig. 6 shows the evolutionary branch map of 25 species ( $P < 0.05$ ). A more concise LEfSe evolutionary branch map was obtained by removing the species with significant differences (Fig. 7). For different species with an LDA score  $> 2$  and significantly high abundance in each group, the top 10 species with the lowest Pvalue are plotted in a bar chart (Fig. 8). The results showed that the different species with significant effects in the treatment groups were as follows: Bacteroidia

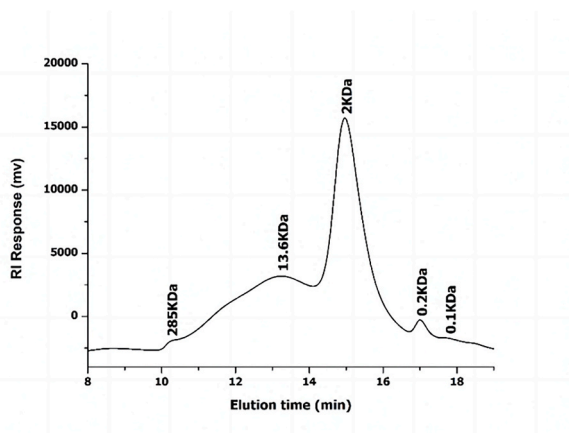
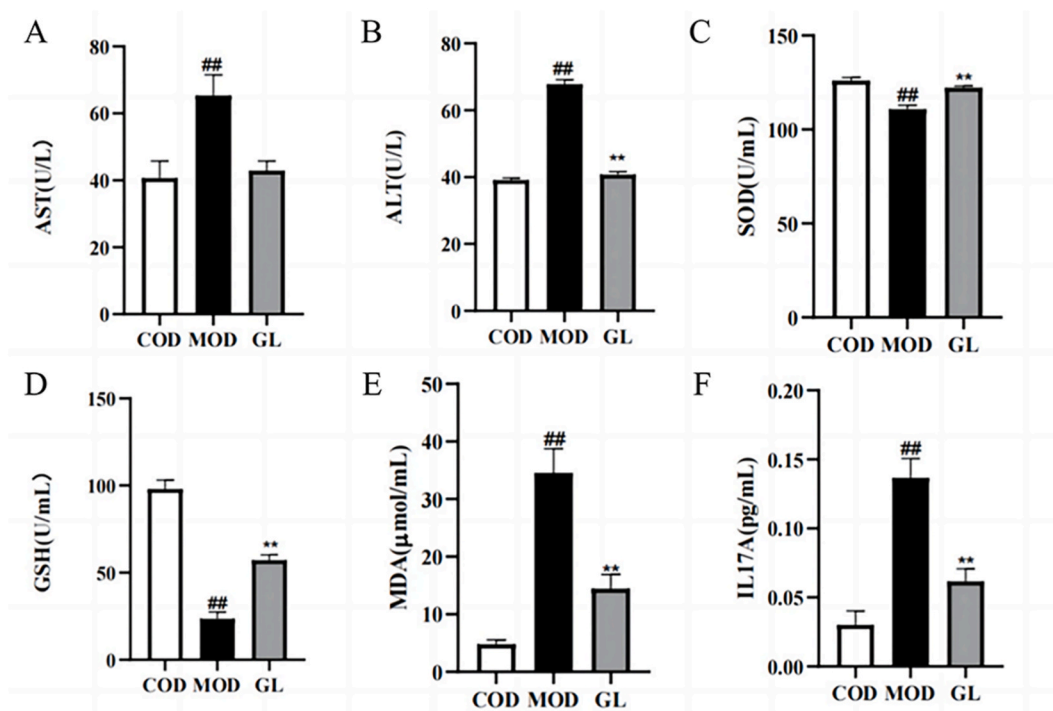


Fig. 2. Hpsc results.

**Table 1**  
Sample retention time and molecular weight.

No.	Retention time (min)	Molecular weight (KDa)
1	10.429	285
2	13.225	13.6
3	14.963	2
4	17.003	0.2



**Fig. 3.** Effects of Ganoderma lucidum polysaccharide on AST, ALT, GSH, SOD, MDA and IL17A levels in drug-induced liver injury mice. **(A)** AST. **(B)** ALT. **(C)** SOD. **(D)** GSH **(E)** MDA. **(F)** IL17A. Notes: CON: Control group; MOD: Model group; GL: Ganoderma lucidum polysaccharide administration group; AST: Aspartate aminotransferase; ALT: Alanine aminotransferase; GSH: Glutathione; SOD: Superoxide dismutase; MDA: Malondialdehyde; IL-17A: Interleukin 17a. Values were presented as the mean  $\pm$  standard deviation (n = 3). #: P < 0.05, ##: P < 0.01, vs. CON; \*: P < 0.05, \*\*: P < 0.01, vs. MOD.

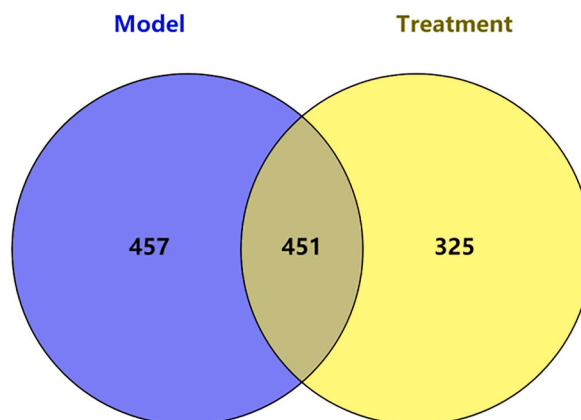


**Fig. 4.** Venn diagram of OTU/ASV distribution comparison.

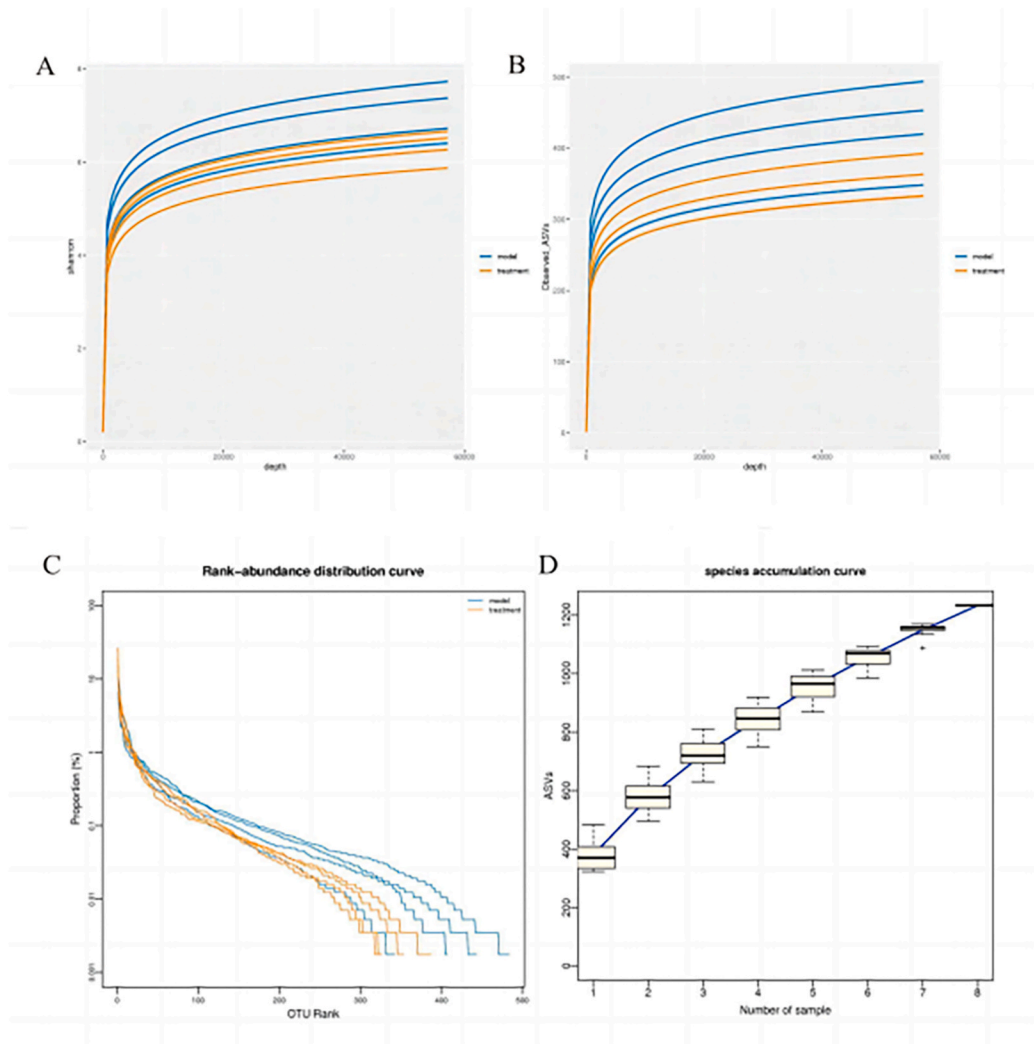


**Fig. 5.** Alpha diversity analysis (A) Shannon-Wiener curve. (B) rarefaction curve. (C) Rank-abundance curve. (D) species accumulation boxplot.

(class level), *Alloprevotella* (genus level), *Prevotellaceae* (family level), *Bacteroidales* (order level), uncultured-Bacteroidales-bacterium (species level), *Bacteroidetes* (phylum level), *Lactobacillus-intestinalis* (species level), *Pasteurellales* (order level), *Pasteurellaceae* (family level), *Staphylococcus-lentus* (species level); The significant difference species in the model group were as follows: *Intestinimonas* (genus level), *Clostridium-XIVa* (genus level), uncultured-bacterium (species level), *Deferribacterales* (family level) and *Deferribacte* (class level), *Deferribacteres* (phylum level), *Pseudoflavonifractor* (phylum level), *Erysipelotrichales*(order level).

### 3.7. Abundance analysis of gut microbiota structure at the phylum level

In this study, we identified and analyzed the microbiota at the phylum, class, order, family and genus levels. At the phylum level, 11 bacterial species accounting for more than 1 % were detected. The phyla level results (Fig. 9) showed that compared with the model group, the treatment group could reduce the species abundance of Firmicutes, Verrucomicrobia and Proteobacteria, and increase the species abundance of Bacteroidetes.

### 3.8. Abundance analysis of gut microbiota structure at genus level

In order to reflect the similarity and difference of species composition at the genus level of samples, we drew the Heatmap map of the 100 species with the highest abundance at the horizontal genus level (Fig. 10A). Metastats analysis compares the samples between groups to find species with significant differences between the two groups at each taxonomic level. With  $p$  value  $< 0.05$  as the significance screening threshold, for species with significant differences in relative abundance between groups, Species with abundance greater than 0.001 in each group were selected for heat maps (Fig. 10B) and box maps (Fig. 10C). The results showed that at the genus

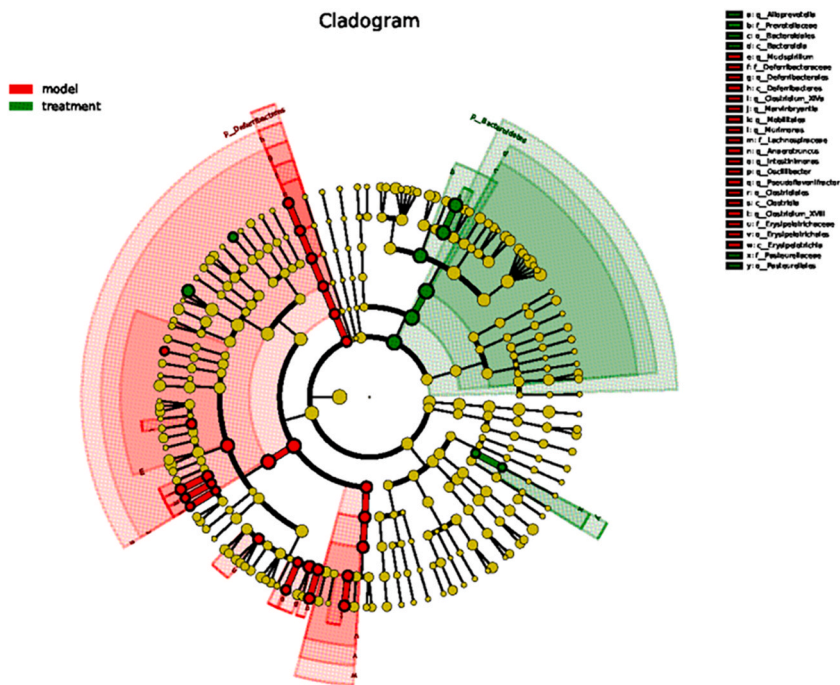


**Fig. 6.** LefSe branching diagram. Note: Different colors represent different groups, nodes represent species with significantly higher relative abundance, and yellow nodes represent species with no significant relative abundance difference between groups; The diameter of the node is proportional to the relative abundance.

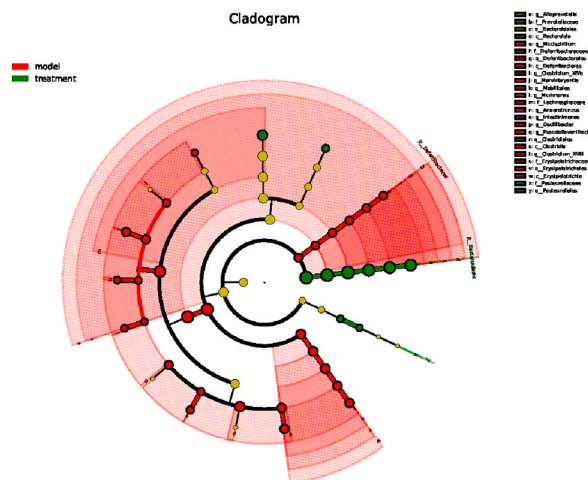


**Fig. 7.** LefSe evolutionary branching plot with non-significantly divergent species removed.

level, compared with the model group, the treatment group was able to reduce the abundance of *Mucispirillum*, *Anaerotruncus*, *Clostridium-XVIII*, *Intestinimonas*, *Pseudoflavonifractor*, *Clostridium-XIVa*, *Oscillibacter*, *Marvinbryantia*, *Clostridium-XIVb*. Increasing the abundance of *Alloprevotella*.

### 3.9. Analysis of microbial $\beta$ diversity

We first calculated the Bray-Cruits dissimilarity matrix between samples, and then averaged linkage hierarchical clustering of samples, with branches that were close to each other between model groups and within treatment groups, indicating that the species composition of samples within groups was similar (Fig. 11A); nonmetric multidimensional scaling (NMDS) can be ordered based on any type of distance and sample (Fig. 11B); PCA principal component analysis was based on OTU/ASV abundance tables, using variance decomposition to reflect differences between samples (Fig. 11C); PCA results showed that PC1 (46.042 %) and PC2 (20.13 %)

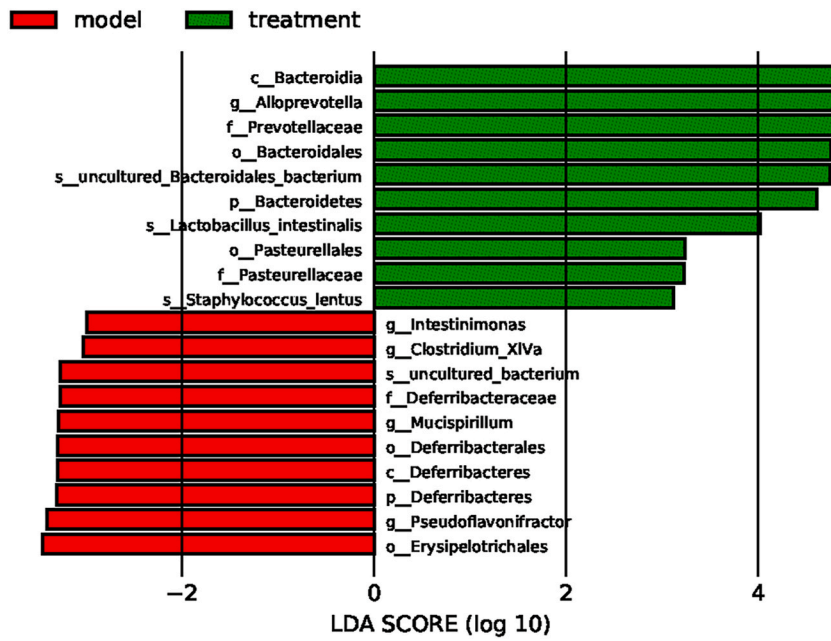


Fig. 8. LDA bar chart.

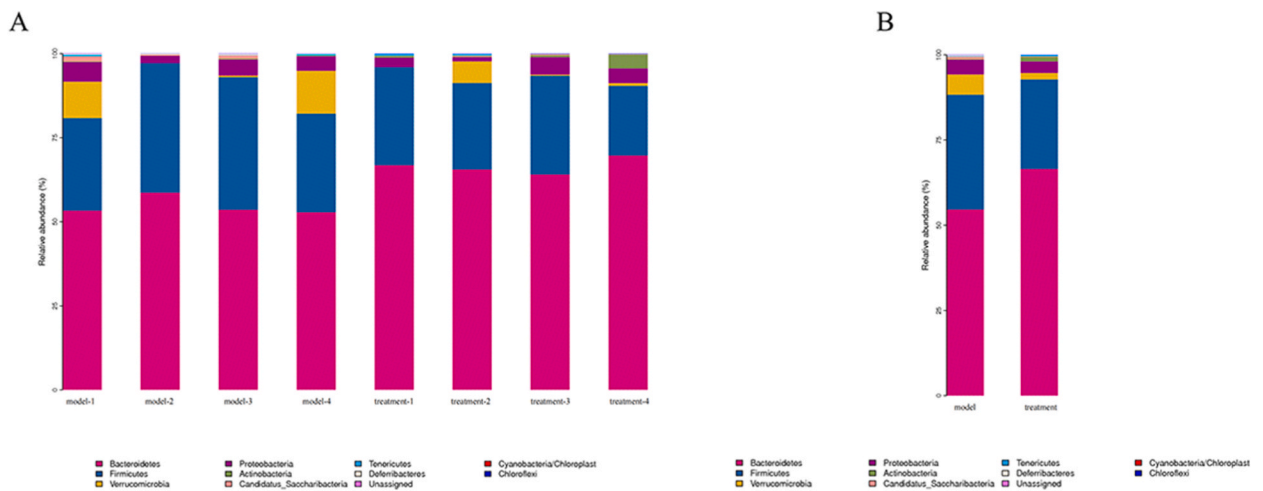


Fig. 9. Horizontal species distribution histogram of phylum. (A) Histogram of species distribution within phyla horizontal group. (B) Histogram of species distribution between phyla horizontal groups.

were significantly separated between the model group and the drug group. PLS-DA (Partial Least squares-discriminant Analysis), that is, partial least squares-discriminant analysis, is a Discriminant Analysis method in multivariate data analysis technology (Fig. 11D). The results showed that the model group and the drug group were far away and the difference was large.

### 3.10. Functional prediction analysis

Welch's T-test was used to compare the differences in the relative abundance of functions in pairwise grouped samples to find out the functions with significant differences between the two groups. The value with  $p < 0.05$  as screening threshold, the significance of difference for the function of the relative abundance of significant differences between groups draw a bar chart (Fig. 12). Through KEGG function prediction of gut microbiota, we identified 13 significant pathways ( $p < 0.05$ ). Among them, D-Glutamine and D-glutamate metabolism were the pathways with the largest average relative abundance in the two groups of samples in the model group and the treatment group, which belonged to metabolism-related pathways.



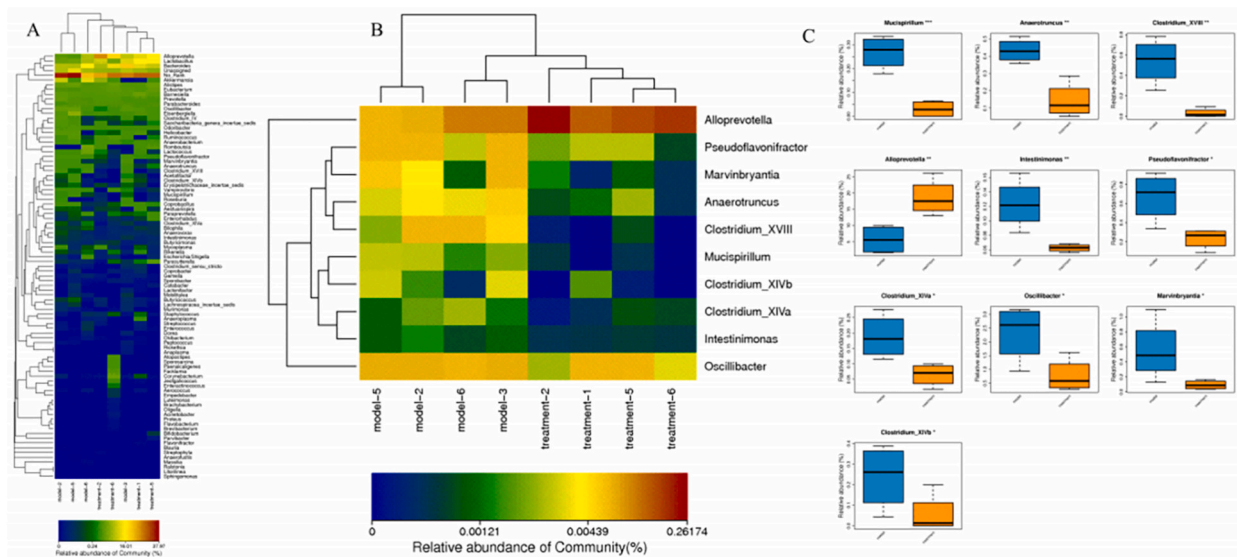


**Fig. 10.** Structural abundance analysis of the bacterial flora at the genus level. **(A)** Genus level Heatmap map. Note: The colors in the figure represent the abundance of the species, with the color changing from blue to red indicating the species abundance from small to large. **(B)** Heatmap of species with significant differences in relative abundance at the genus level. **(C)** box plot of species comparison at the genus level (\* =  $P < 0.05$ , \*\* =  $P < 0.01$ , \*\*\* =  $P < 0.001$ ).

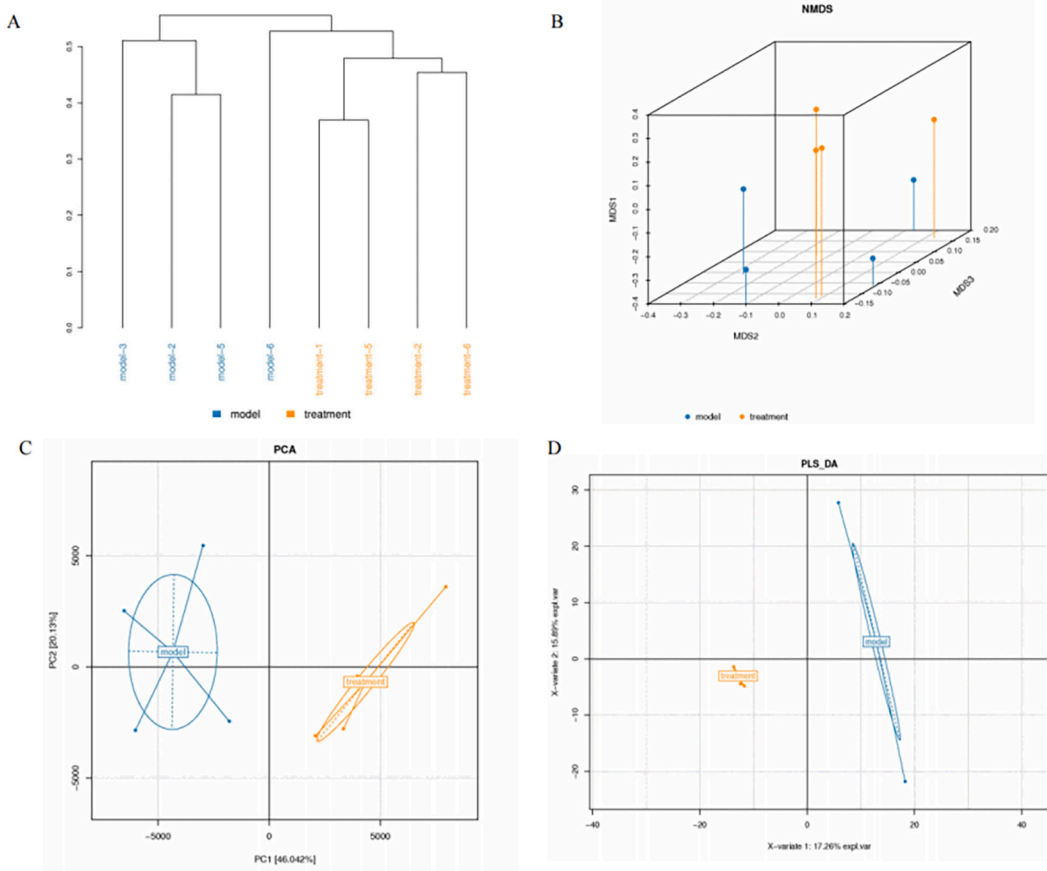


**Fig. 11.** Analysis of  $\beta$  diversity. **(A)** sample cluster tree diagram. **(B)** NMDS analysis diagram. **(C)** PCA diagram. **(D)** PLS\_DA diagram.

#### 4. Discussion

The liver is a critically important organ for the regulation of metabolic homeostasis [23,24]. Acute liver injury (ALI) is one of the most prominent causes of liver disease and poses a serious threat to the lives and health of patients [25,26]. An increasing number of studies have shown a close link between gut microbiota and liver injury, and gut microbiota has been shown to modulate many extraintestinal organ diseases, including liver injury [27,28]. Intestinal mucosal barrier is the first barrier of human body contact with exogenous substances, the lymphocytes in the intestinal mucosa can in the gut and migration between the liver and the defense against pathogens, maintain normal physiological activities of the intestine and liver.

Although the research of *Ganoderma lucidum* in liver diseases has been gradually deepened in recent years [29–31], there is still a lack of elucidating the effect of *Ganoderma lucidum* polysaccharide on liver through intestinal flora. The innovation of this study is to explore the liver protection effect of *Ganoderma lucidum* polysaccharide from the direction of intestinal flora through 16S rRNA sequencing. In this study, we investigated the effects of *Ganoderma lucidum* polysaccharides on alleviating the severity of acute liver injury by improving the diversity and function of gut microbiota using an acute liver injury model.

According to the results of oxidative and inflammatory indexes in mouse liver tissue, *Ganoderma lucidum* polysaccharide can promote the proliferation of mouse intestinal epithelial cells and resist oxidative stress injury to maintain the integrity of mucosal barrier [32,33], thereby improving the intestinal mucosal inflammation and CCl<sub>4</sub>-induced acute liver injury in mice.

LEfSe analysis identified 20 significant species. The results showed that the different species with significant effects in the treatment groups were as follows: Bacteroidia (class level), Alloprevotella (genus level), Prevotellaceae (family level), Bacteroidales (order level), uncultured-Bacteroidales-bacterium (species level), Bacteroidetes (phylum level), Lactobacillus-intestinalis (species level), Pasteurellales (order level), Pasteurellaceae (family level), Staphylococcus-lentus (species level); The differential species with significant effects in the model group were: Intestinimonas (genus level), Clostridium-XIVa (genus level), uncultured-bacterium (species level), Deferribacterales (family level), Deferribacte (class level), Deferribacteres (phylum level), Pseudoflavonifractor (phylum level), Erysipelotrichales (order level). Among them, Bacteroidia at the class level showed the most significant difference in the treatment groups. The most significant difference in the model group was for Erysipelotrichales at the order level.

A total of 11 species were detected, accounting for more than 1 % of the gut microbiota. Compared with the model group, the species abundance of Firmicutes, Verrucomicrobia and Proteobacteria in the treatment group was lower, and that of Bacteroidetes was higher. Firmicutes in mice are involved in a variety of carbohydrate metabolic pathways [34,35], while Bacteroidetes had a high functional diversity. It can effectively promote polysaccharide degradation [36]. Using a p-value <0.05 as the threshold for significance screening, 10 species with an abundance greater than 0.001 in each group were selected. Compared with the model group, *Ganoderma lucidum* polysaccharide can reduce the abundance of Mucispirillum, Anaerotruncus, Clostridium-XVIII, Intestinimonas, Pseudoflavonifractor, Clostridium-XIVa, Oscillibacter, Marvinbryantia, Clostridium-XIVb. Increasing the abundance of Alloprevotella, Anaerotruncus, Clostridium-XVIII, Intestinimonas, Pseudoflavonifractor, Clostridium-XIVa, Oscillibacter, Marvinbryantia, Clostridium-XIVb belongs to the taxonomic group Firmicutes. Mucispirillum belongs to Deferribacteres in the taxonomy. Alloprevotella belongs to Bacteroidetes in the taxonomy.

Deferribacteres can regulate gut microbiota [37,38], Firmicutes and Bacteroidetes are the major phyla in humans, and 90 % of

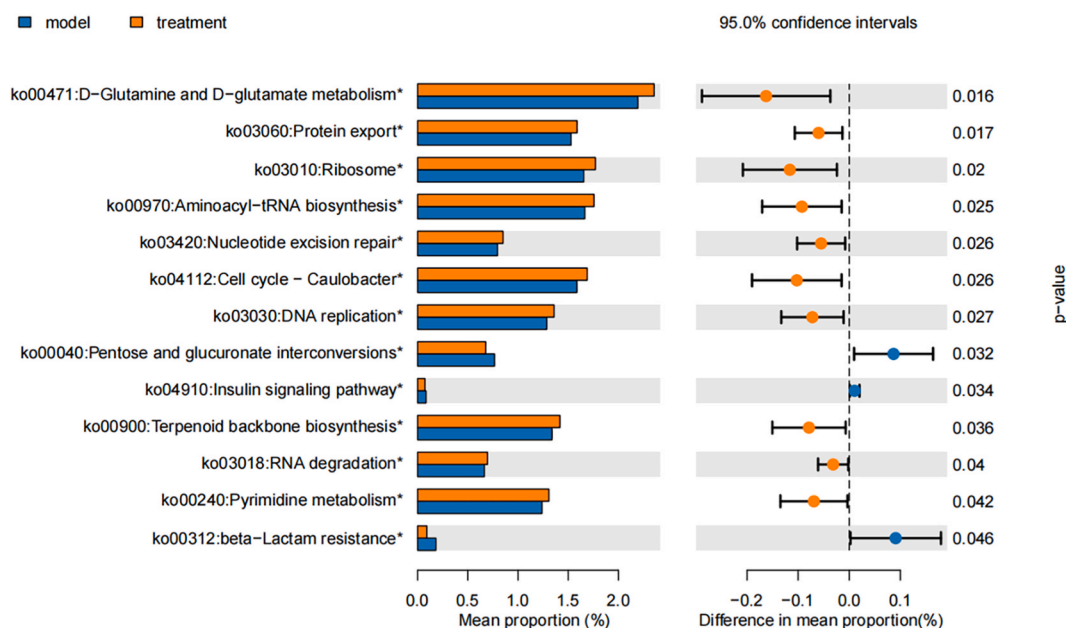


Fig. 12. Comparison of KEGG pathway difference analysis between model group and treatment group.

Firmicutes are Gram-positive bacteria [39]. The decrease in Firmicutes is consistent with the findings of Chen T. Firmicutes is also reduced in the gut microbiota of patients with chronic liver disease and hepatocellular carcinoma [40]. *Ganoderma lucidum* polysaccharide can reduce the ratio of Firmicutes to Bacteroidetes. Firmicutes/Bacteroidetes(F/B) can not only affect intestinal homeostasis, but also cause fatty liver injury [41,42]. In addition, some researchers have pointed out that *Ganoderma lucidum* mycelium can reduce the ratio of Firmicutes to Bacteroidetes and the level of Proteobacteria carrying endotoxins, maintain the integrity of the intestinal barrier and reduce metabolic endotoxemia [43], which is consistent with our findings.

## 5. Conclusions

In conclusion, *Ganoderma lucidum* polysaccharide can improve CCl<sub>4</sub>-induced acute liver injury and intestinal flora imbalance in mice, which explains the liver protective effect of *Ganoderma lucidum* polysaccharide from the perspective of intestinal flora. The pharmacological effect of *Ganoderma lucidum* polysaccharide is complex, and its hepatoprotective mechanism needs further comprehensive and in-depth research. This experiment provides experimental and theoretical support for the further development of functional food and drug based on *Ganoderma lucidum*.

## Ethics statement

Animal experiments were approved by the Animal Ethics Committee of Beihua University(BHAH20220098), and animal procedures were strictly carried out according to the legislation for care and use of laboratory animals of China.

## Data availability

Data will be made available on request.

## CRediT authorship contribution statement

**Xiao-tian Zhang:** Writing – review & editing, Writing – original draft, Resources, Funding acquisition, Data curation, Conceptualization. **Yue Yang:** Writing – original draft, Funding acquisition, Data curation. **Chunlei Ji:** Supervision, Methodology, Conceptualization. **Yujuan Fu:** Visualization, Methodology, Investigation. **Xinyi Pu:** Visualization, Methodology, Investigation. **Guangyu Xu:** Writing – review & editing, Writing – original draft, Resources, Project administration, Methodology, Funding acquisition, Data curation, Conceptualization.

## Declaration of competing interest

The authors declare that they have no known competing financial interests or personal relationships that could have appeared to influence the work reported in this paper.

## Acknowledgments

This work was funded by special project of medical and health talents in Jilin Province (2019SRCJ021), National Natural Science Foundation of China (82102401), National Natural Science Foundation of China (81973371).

## References

- [1] C. Dai, X. Xiao, D. Li, S. Tun, Y. Wang, T. Velkov, et al., Chloroquine ameliorates carbon tetrachloride-induced acute liver injury in mice via the concomitant inhibition of inflammation and induction of apoptosis, *Cell Death & Disease* 9 (2018), <https://doi.org/10.1038/s41419-018-1136-2>.
- [2] S. Gong, Y. Feng, Y. Zeng, H. Zhang, M. Pan, F. He, et al., Gut microbiota accelerates cisplatin-induced acute liver injury associated with robust inflammation and oxidative stress in mice, *J. Transl. Med.* 19 (2021), <https://doi.org/10.1186/s12967-021-02814-5>.
- [3] X. Li, X. Liu, Y. Zhang, C. Cheng, J. Fan, J. Zhou, et al., Hepatoprotective effect of apolipoprotein A4 against carbon tetrachloride induced acute liver injury through mediating hepatic antioxidant and inflammation response in mice, *Biochem. Biophys. Res. Commun.* 534 (2021) 659–665, <https://doi.org/10.1016/j.bbrc.2020.11.024>.
- [4] C. Chen, T. Lu, P. Chen, Z. Li, Y. Yang, S. Fan, et al., Cyclization strategy leads to highly potent bromodomain and extra-terminal (BET) bromodomain inhibitors for the treatment of acute liver injury, *Eur. J. Med. Chem.* 247 (2023) 115023, <https://doi.org/10.1016/j.ejmech.2022.115023>.
- [5] S. Gong, T. Lan, L. Zeng, H. Luo, X. Yang, N. Li, et al., Gut microbiota mediates diurnal variation of acetaminophen induced acute liver injury in mice, *J. Hepatol.* 69 (2018) 51–59, <https://doi.org/10.1016/j.jhep.2018.02.024>.
- [6] T. Chen, R. Li, P. Chen, Gut microbiota and chemical-induced acute liver injury, *Front. Physiol.* 12 (2021), <https://doi.org/10.3389/fphys.2021.688780>.
- [7] Z. Ren, Y. Huo, Q. Zhang, S. Chen, H. Lv, L. Peng, et al., Protective effect of lactiplantibacillus Plantarum 1201 combined with galactooligosaccharide on carbon tetrachloride-induced acute liver injury in mice, *Nutrients* 13 (2021) 4441, <https://doi.org/10.3390/nu13124441>.
- [8] S. Gong, T. Lan, L. Zeng, H. Luo, X. Yang, N. Li, et al., Gut microbiota mediates diurnal variation of acetaminophen induced acute liver injury in mice, *J. Hepatol.* 69 (2018) 51–59, <https://doi.org/10.1016/j.jhep.2018.02.024>.
- [9] J.-K. Yan, C. Wang, T.-T. Chen, J. Zhu, X. Chen, L. Li, et al., A pectic polysaccharide from fresh okra (*Abelmoschus esculentus* L.) beneficially ameliorates CCl<sub>4</sub>-induced acute liver injury in mice by antioxidant, inhibition of inflammation and modulation of gut microbiota, *Food Chem. Toxicol.* 171 (2023) 113551, <https://doi.org/10.1016/j.fct.2022.113551>.
- [10] X. Xu, S. Liu, Y. Zhao, M. Wang, L. Hu, W. Li, et al., Combination of *Houttuynia cordata* polysaccharide and *Lactiplantibacillus plantarum* P101 alleviates acute liver injury by regulating gut microbiota in mice, *J. Sci. Food Agric.* 102 (2022) 6848–6857, <https://doi.org/10.1002/jsfa.12046>.

- [11] Q. Zou, N. Wang, Z. Gao, H. Xu, G. Yang, T. Zhang, et al., Antioxidant and hepatoprotective effects against acute CCl<sub>4</sub>-induced liver damage in mice from red-fleshed Apple flesh flavonoid extract, *J. Food Sci.* 85 (2020) 3618–3627, <https://doi.org/10.1111/1750-3841.15454>.
- [12] A. Rašković, I. Milanović, N. Pavlović, T. Čebović, S. Vukmirović, M. Mikov, Antioxidant activity of Rosemary (*Rosmarinus officinalis* L.) essential oil and its hepatoprotective potential, *BMC Compl. Alternative Med.* 14 (2014), <https://doi.org/10.1186/1472-6882-14-225>.
- [13] H.-F. Chiu, H.-Y. Fu, Y.-Y. Lu, Y.-C. Han, Y.-C. Shen, K. Venkatakrishnan, et al., Triterpenoids and polysaccharide peptides-enriched *ganoderma lucidum*: a randomized, double-blind placebo-controlled crossover study of its antioxidation and hepatoprotective efficacy in healthy volunteers, *Pharmaceut. Biol.* 55 (2017) 1041–1046, <https://doi.org/10.1080/13880209.2017.1288750>.
- [14] Y.-S. Chen, Q.-Z. Chen, Z.-J. Wang, C. Hua, Anti-inflammatory and hepatoprotective effects of *ganoderma lucidum* polysaccharides against carbon tetrachloride-induced liver injury in Kunming mice, *Pharmacology* 103 (2019) 143–150, <https://doi.org/10.1159/000493896>.
- [15] C. Guo, D. Guo, L. Fang, T. Sang, J. Wu, C. Guo, et al., *Ganoderma lucidum* polysaccharide modulates gut microbiota and immune cell function to inhibit inflammation and tumorigenesis in colon, *Carbohydrate Polymers* 267 (2021) 118231, <https://doi.org/10.1016/j.carbpol.2021.118231>.
- [16] M. Li, L. Yu, Q. Zhai, C. Chu, S. Wang, J. Zhao, et al., Combined *Ganoderma lucidum* polysaccharide and ciprofloxacin therapy alleviates *Salmonella enterica* infection, protects the intestinal barrier, and regulates gut microbiota, *Food Funct.* 14 (15) (2023 Jul 31) 6896–6913, <https://doi.org/10.1039/d3fo00625e>.
- [17] Y. Wang, J. Xiao, Y. Duan, M. Miao, B. Huang, J. Chen, et al., *Lycium barbarum* polysaccharide ameliorates sjögren's syndrome in a murine model, *Mol. Nutr. Food Res.* 65 (11) (2021 Jun) e2001118, <https://doi.org/10.1002/mnfr.202001118>.
- [18] M. Ruart, L. Chavarria, G. Camprecios, N. Suárez-Herrera, C. Montironi, S. Guixé-Muntet, et al., Impaired endothelial autophagy promotes liver fibrosis by aggravating the oxidative stress response during acute liver injury, *J. Hepatol.* 70 (3) (2019 Mar) 458–469, <https://doi.org/10.1016/j.jhep.2018.10.015>.
- [19] B.Y. Yang, X.Y. Zhang, S.W. Guan, Z.C. Hua, Protective effect of procyanidin B2 against CCl<sub>4</sub>-induced acute liver injury in mice, *Molecules* 20 (7) (2015 Jul 3) 12250–12265, <https://doi.org/10.3390/molecules200712250>.
- [20] G. Xu, X. Lv, Y. Feng, H. Li, C. Chen, H. Lin, et al., Study on the effect of active components of *Schisandra chinensis* on liver injury and its mechanisms in mice based on network pharmacology, *Eur. J. Pharmacol.* 910 (2021) 174442, <https://doi.org/10.1016/j.ejphar.2021.174442>.
- [21] W.-W. Lu, T.-X. Fu, Q. Wang, Y.-L. Chen, T.-Y. Li, G.-L. Wu, The effect of total glucoside of paeyon on gut microbiota in nod mice with Sjögren's syndrome based on high-throughput sequencing of 16S rRNA gene, *Chin. Med.* 15 (2020), <https://doi.org/10.1186/s13020-020-00342-w>.
- [22] W. Liu, R. Zhang, R. Shu, J. Yu, H. Li, H. Long, et al., Study of the relationship between microbiome and colorectal cancer susceptibility using 16S rRNA sequencing, *BioMed Res. Int.* 2020 (2020) 1–17, <https://doi.org/10.1155/2020/7828392>.
- [23] R. Zhu, G. Zeng, Y. Chen, Q. Zhang, B. Liu, J. Liu, et al., Oroxylin a accelerates liver regeneration in CCl<sub>4</sub>-induced acute liver injury mice, *PLoS One* 8 (2013), <https://doi.org/10.1371/journal.pone.0071612>.
- [24] E. Trefts, M. Gannon, D.H. Wasserman, The liver, *Curr. Biol.* 27 (2017), <https://doi.org/10.1016/j.cub.2017.09.019>.
- [25] Y. Li, Z. Guo, H. Cui, T. Wang, Y. Xu, J. Zhao, Urantide prevents CCl<sub>4</sub>-induced acute liver injury in rats by regulating the MAPK signalling pathway, *Mol. Med. Rep.* 24 (2021), <https://doi.org/10.3892/mmr.2021.12329>.
- [26] X. Zhang, G. Kuang, J. Wan, R. Jiang, L. Ma, X. Gong, et al., Salidroside protects mice against CCl<sub>4</sub>-induced acute liver injury via down-regulating CYP2E1 expression and inhibiting NLRP3 inflammasome activation, *Int. Immunopharm.* 85 (2020) 106662, <https://doi.org/10.1016/j.intimp.2020.106662>.
- [27] H. Liang, H. Song, X. Zhang, G. Song, Y. Wang, X. Ding, et al., Metformin attenuated sepsis-related liver injury by modulating gut microbiota, *Emerg. Microb. Infect.* 11 (2022) 815–828, <https://doi.org/10.1080/22221751.2022.2045876>.
- [28] Y. Li, H. Hu, H. Yang, A. Lin, H. Xia, X. Cheng, et al., Vine tea (*Ampelopsis grossedentata*) extract attenuates CCl<sub>4</sub>-induced liver injury by restoring gut microbiota dysbiosis in mice, *Mol. Nutr. Food Res.* 66 (2022) 2100892, <https://doi.org/10.1002/mnfr.202100892>.
- [29] Y.S. Chen, Q.Z. Chen, Z.J. Wang, C. Hua, Anti-inflammatory and hepatoprotective effects of *ganoderma lucidum* polysaccharides against carbon tetrachloride-induced liver injury in Kunming mice, *Pharmacology* 103 (3–4) (2019) 143–150, <https://doi.org/10.1159/000493896>.
- [30] C. Chen, J. Chen, Y. Wang, L. Fang, C. Guo, T. Sang, H. Peng, Q. Zhao, S. Chen, X. Lin, X. Wang, *Ganoderma lucidum* polysaccharide inhibits HSC activation and liver fibrosis via targeting inflammation, apoptosis, cell cycle, and ECM-receptor interaction mediated by TGF- $\beta$ /Smad signaling, *Phytomedicine* 110 (2023 Feb) 154626, <https://doi.org/10.1016/j.phymed.2022.154626>.
- [31] G.L. Zhang, Y.H. Wang, W. Ni, H.L. Teng, Z.B. Lin, Hepatoprotective role of *Ganoderma lucidum* polysaccharide against BCG-induced immune liver injury in mice, *World J. Gastroenterol.* 8 (4) (2002 Aug) 728–733, <https://doi.org/10.3748/wjg.v8.i4.728>.
- [32] M.E. Meneses, D. Martínez-Carrera, L. González-Ibáñez, N. Torres, M. Sánchez-Tapia, C.C. Márquez-Mota, et al., Effects of Mexican *ganoderma lucidum* extracts on liver, kidney, and the gut microbiota of wistar rats: a repeated dose oral toxicity study, *PLoS One* 18 (2023), <https://doi.org/10.1371/journal.pone.0283605>.
- [33] T. Sang, C. Guo, D. Guo, J. Wu, Y. Wang, Y. Wang, et al., Suppression of obesity and inflammation by polysaccharide from sporoderm-broken spore of *ganoderma lucidum* via gut microbiota regulation, *Carbohydrate Polymers* 256 (2021) 117594, <https://doi.org/10.1016/j.carbpol.2020.117594>.
- [34] X. Wang, H. Liu, Y. Li, S. Huang, L. Zhang, C. Cao, et al., Altered gut bacterial and metabolic signatures and their interaction in gestational diabetes mellitus, *Gut Microb.* 12 (2020) 1840765, <https://doi.org/10.1080/19490976.2020.1840765>.
- [35] B. Xue, J. Xie, J. Huang, L. Chen, L. Gao, S. Ou, et al., Plant polyphenols alter a pathway of energy metabolism by inhibiting fecal bacteroidetes and Firmicutes in vitro, *Food & Function* 7 (2016) 1501–1507, <https://doi.org/10.1039/c5fo01438g>.
- [36] R.P. Singh, Glycan utilisation system in bacteroides and bifidobacteria and their roles in gut stability and health, *Appl. Microbiol. Biotechnol.* 103 (2019) 7287–7315, <https://doi.org/10.1007/s00253-019-10012-z>.
- [37] P. Pushpanathan, G.S. Mathew, S. Selvarajan, K.G. Seshadri, P. Srikanth, Gut microbiota and its mysteries, *Indian J. Med. Microbiol.* 37 (2019) 268–277, [https://doi.org/10.4103/ijmm.ijmm\\_19\\_373](https://doi.org/10.4103/ijmm.ijmm_19_373).
- [38] J. Duan, X. Meng, S. Liu, P. Zhou, C. Zeng, C. Fu, et al., Gut microbiota composition associated with clostridium difficile-positive diarrhea and *C. difficile* type in ICU patients, *Front. Cell. Infect. Microbiol.* 10 (2020), <https://doi.org/10.3389/fcimb.2020.00190>.
- [39] C.O. Jasirwan, A. Muradi, I. Hasan, M. Simadibrata, I. Rinaldi, Correlation of gut Firmicutes/Bacteroidetes ratio with fibrosis and steatosis stratified by body mass index in patients with non-alcoholic fatty liver disease, *Bioscience of Microbiota, Food and Health* 40 (2021) 50–58, <https://doi.org/10.12938/bmfh.2020-046>.
- [40] T. Chen, R. Ding, X. Chen, Y. Lu, J. Shi, Y. Lü, et al., Firmicutes and blautia in gut microbiota lessened in chronic liver diseases and hepatocellular carcinoma patients: a pilot study, *Bioengineered* 12 (2021) 8233–8246, <https://doi.org/10.1080/21655979.2021.1982273>.
- [41] N.Y. Lee, S.J. Yoon, D.H. Han, H. Gupta, G.S. Youn, M.J. Shin, et al., *Lactobacillus* and *pediococcus* ameliorate progression of non-alcoholic fatty liver disease through modulation of the gut microbiome, *Gut Microb.* 11 (2020) 882–899, <https://doi.org/10.1080/19490976.2020.1712984>.
- [42] H.-X. Liu, Y. Hu, Y.-J.Y. Wan, Microbiota and bile acid profiles in retinoic acid-primed mice that exhibit accelerated liver regeneration, *Oncotarget* 7 (2015) 1096–1106, <https://doi.org/10.18632/oncotarget.6665>.
- [43] C.J. Chang, C.S. Lin, C.C. Lu, J. Martel, Y.F. Ko, D.M. Ojcius, S.F. Tseng, T.R. Wu, Y.Y. Chen, J.D. Young, H.C. Lai, *Ganoderma lucidum* reduces obesity in mice by modulating the composition of the gut microbiota, *Nat. Commun.* 6 (2015 Jun 23) 7489, <https://doi.org/10.1038/ncomms8489>.